ISBN: 978-3-95450-132-8 doi:10.18429/JACoW-IPAC2014-MOPRI109

HIGH-POWER PROTON-SYNCHROTRON COLLIMATION STUDIES

A. Alekou, Y. Papaphilippou, CERN, Geneva, Switzerland
D. Spitzbart, TU Vienna, Wien, Austria

Abstract

The High-Power Proton-Synchrotron (HP-PS) will be delivering a 2 MW proton beam to a fixed target in order to produce neutrinos within the LAGUNA-LBNO project. A mechanical collimation system is essential to prevent lost particles from hitting the super-feric dipoles of the HP-PS ring and to also limit the equipment irradiation close to the beam. This paper presents how the efficiency of the HP-PS collimator system is optimised with respect to the change of the collimators' thickness, material and beam halo size.

INTRODUCTION

The High-Power Proton-Synchrotron (HP-PS) [1], which is at its final design stage, will be delivering a 2 MW proton beam to a fixed target at CERN, for neutrino experiments within the LAGUNA-LBNO project [2]. The collimation system is essential for machine protection, in general. In particular it is mandatory for protecting super-conducting magnets from quenching.

The HP-PS has a 3-fold symmetry and provides a long straight section solely for beam collimation. A two-stage collimation system has been designed, that uses a thin primary collimator (scatterer) as a means to give an angle-increase to the halo particles it intercepts, and a secondary collimator as an absorber for those scattered particles. In order to find the optimum collimation settings, numerous parameters have been varied, including the collimators' thickness, material and beam halo size. This paper presents the main results and describes the steps to be followed in the immediate future.

COLLIMATOR AND BEAM-HALO SETTINGS

Collimator-settings

The optimum locations of the collimators in a two-stage transverse collimation system are given by [3]:

$$\begin{aligned} \mu_{s,1} &= \cos^{-1}(N_p/N_s) \\ \mu_{s,2} &= \pi - \mu_{s,1} \end{aligned} \quad (1)$$

where $\mu_{s,1}$, $\mu_{s,2}$ are the phase advances of the first and second secondary collimators with respect to the primary, and N_p, N_s are the jaw opening sizes of the primary and secondary collimators, respectively, in number of σ, the geometrical r.m.s. beam size.

Various jaw opening sizes were considered for the collimators; the results described in this paper are those obtained for $N_p = 3\sigma$ and $N_s = 3.5\sigma$ that correspond to $\mu_{s,1} = 31^o$ and $\mu_{s,2} = 149^o$ respectively. Note that both horizontal (H) and vertical (V) collimators were used. Throughout the HP-PS collimation system studies it has been shown that the collimation system performance is significantly enhanced when there are no quadrupoles between the primary and secondary collimators. It has also been demonstrated that additional collimators at $\mu = 90^o$ improve the efficiency. Although Eq. 1 describes the optimum collimation-positioning with respect to the primary collimator, the final placement of the collimators presented here has been adjusted according to the results of tracking studies. It should be emphasised that the optics of the HP-PS sequence imposed in many cases the location and thickness of the secondary collimators. The optimum and used locations and phase advances of the secondary collimators, with respect to the primaries, are shown in Table 1.

Table 1: Optimum and used locations and phase advance of the collimators. H: Horizontal, V: Vertical, P: Primary, S: Secondary, ADD: Additional

Collimator	Opt-s [m]	Used-μ [^{o}]	Used-s [m]
HP	-	336.98	0.00
VP	-	337.00	0.00
HS1	350.81	33.89	351.87
VS1	352.00	34.4	353.87
HS2	422.58	141.48	420.49
VS2	392.35	138.67	388.00
H.ADD1	400.40	71.92	385.00
V.ADD1	373.39	59.59	364.00

The SixTrack [4] tracking code was used for halo production and tracking. The characteristics incorporated by this software regarding collimation studies are listed in [5].

Three different collimator-materials were simulated with SixTrack: graphite (C), copper (Cu) and tungsten (W). It was shown that the collimation-performance was good only for a narrow range of very small thicknesses of the order of μm when using tungsten or copper for primary collimators. On the contrary, graphite was performing well for a wide range of larger thicknesses of the order of mm and was therefore selected to be the material of the primary collimators.

Fig. 1 presents the inefficiency, defined as $\eta_{inef} = N_{lost}/N_{abs}$, where N_{lost} is the number of particles that impacted the aperture (lost) and N_{abs} the number of those absorbed by the collimators, as a function of the impact parameter (transverse offset between the impact location on a collimator and the edge of its jaw) for different materials of the secondary collimators. It can be seen that tungsten results in a smaller inefficiency and is therefore selected as the material for the secondary collimators.

By scanning the efficiency for different thicknesses of the primary collimators, the optimum thickness was found to be

Content from this work may be used under the terms of the CC BY 3.0 licence (© 2014). Any distribution of this work must maintain attribution to the author(s), title of the work, publisher, and DOI.

ISBN: 978-3-95450-132-8 doi:10.18429/JACoW-IPAC2014-MOPRI109

Content from this work may be used under the terms of the CC BY 3.0 licence (© 2014). Any distribution of this work must maintain attribution to the author(s), title of the work, publisher, and DOI.

~12 mm; the first secondary collimators were set to to 2 m of thickness whereas all other collimators to 1 m.

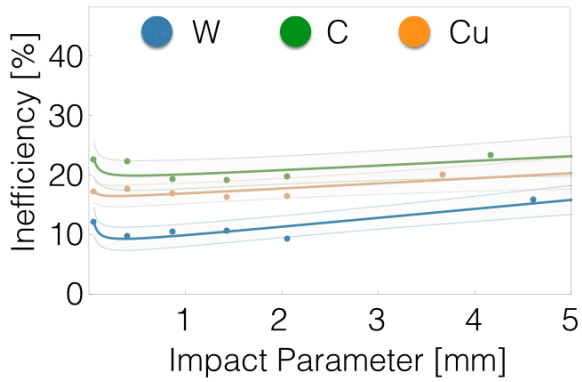

Figure 1: Inefficiency of the collimator system with respect to different impact parameters for different materials of the secondary collimators.

Halo-parameters

Horizontal and vertical halos of 2,000 particles, with a thickness (smear) of 0.016σ and reference energy of 4 GeV, were generated directly upstream the primary horizontal collimator at 3.2σ. Note that using both horizontal and vertical halos with particles occupying the largest possible horizontal and vertical phase-space is one of the worst-case scenarios. The horizontal and vertical normalised emittances were $\epsilon_{x,n} = 8\ \mu m \cdot rad$ and $\epsilon_{x,n} = 15.5\ \mu m \cdot rad$ respectively.

Fig. 2 presents how the inefficiency changes with the size of beam-halo. It can be seen that the lowest inefficiency is obtained when using halo=3.3σ, and that for halo values closer to the aperture of the secondary collimators there is a significant increase in the inefficiency.

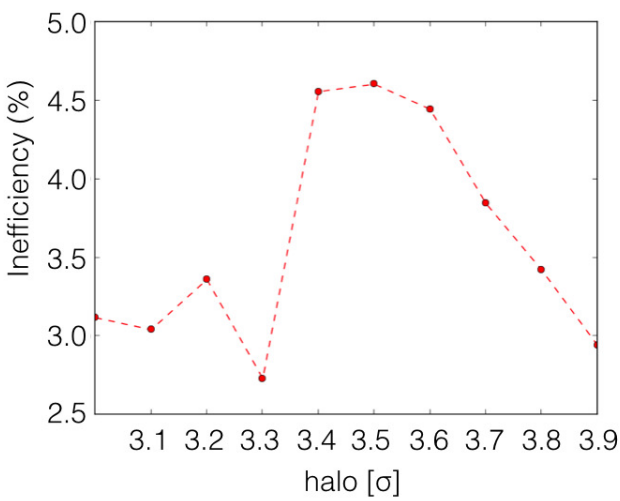

Figure 2: Inefficiency with respect to the halo size.

COLLIMATION EFFICIENCY

In the top of Fig. 3, the power deposition per meter is presented caused by particles that have not been absorbed by the collimation system but instead impacted the magnets' aperture (lost particles), while in the bottom part, the locations of the losses are shown with respect to the ring elements. Most of the particles are lost between $17<s<19$ m. Since it is expected that most losses will occur at injection, it has been calculated that each particle corresponds to 0.8 W. Taking into account the radiation limit of 1 W/m it can be seen that this limit is exceeded in a few locations. The tracks of the particles lost between $17<s<19$ m, shown in Fig. 4, reveal that these losses occur due to the increase of the particles' angles after impacting the secondary collimators.

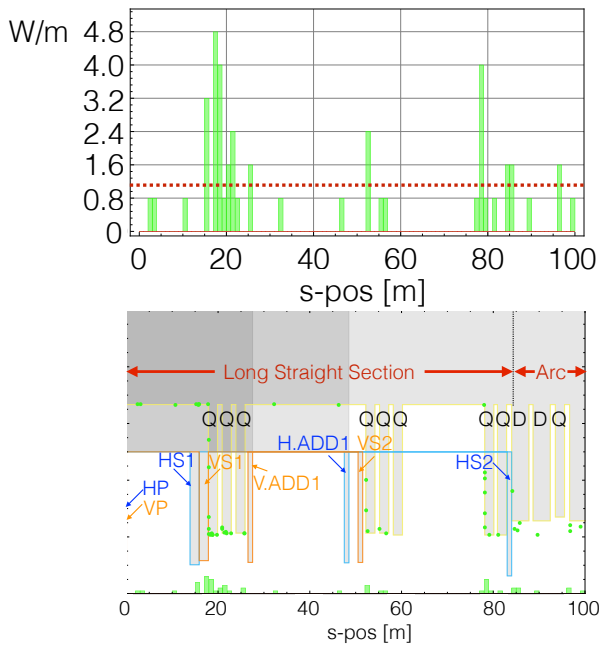

Figure 3: Top: power deposition per meter on the aperture by impacted (lost) particles. The horizontal red line represents the 1 W/m limit. Bottom: location of lost particles with respect to the position of collimators (blue/orange: horizontal/vertical), quadrupoles (Q) and dipoles (D).

The efficiency of each collimator, defined as the number of absorbed particles divided by the total number of particles, is listed in Table 2. The majority of particles is absorbed by the first secondary collimator, HS1. Although the first vertical secondary collimator, VS1, seems to be absorbing fewer particles in comparison to HS1, studies have shown that when this collimator is not present, the power deposition per meter at several locations doubles.

Fig. 5 presents the power deposition along the collimation long straight section when using a 3.3σ halo (horizontal and vertical). Although the losses for $17<s<19$ m have been increased, compared to Fig. 3 (top) where a 3.3σ halo was inputted, there are now fewer areas in which the power deposition exceeds the 1 W/m limit. Special "masks" can be used to protect the quadrupoles located at ~20 m (see Fig. 3, bot-

ISBN: 978-3-95450-132-8 doi:10.18429/JACoW-IPAC2014-MOPRI109

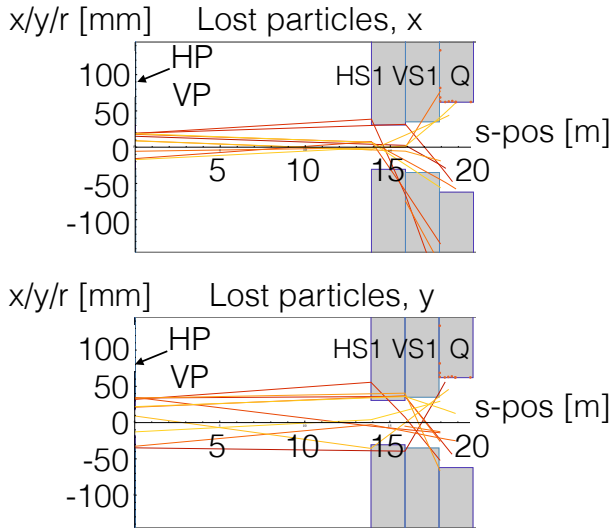

Figure 4: x- and y- coordinates (top and bottom respectively) of the particles lost between 17-19 m. The primary and first secondary collimators are shown, together with the first focusing quadrupole (Q).

Table 2: Efficiency (in %) of Each Collimator

Collimator	Efficiency (%)
HP	2.30
VP	0.75
HS1	71.98
VS1	7.90
HS2	2.30
VS2	4.20
H.ADD.1	5.55
V.ADD.1	1.50

tom), but already further work is ongoing aiming to reduce the power deposition within this specific area.

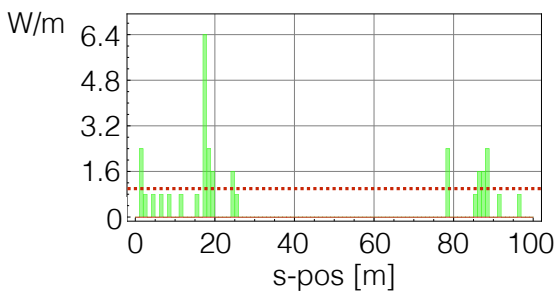

Figure 5: Power deposition per meter on the aperture by impacted (lost) particles for 3.3σ halo. The horizontal red line represents the 1 W/m limit.

LONGITUDINAL COLLIMATION

Longitudinal collimation studies have been initiated. A primary collimator has been placed in the arc upstream the long straight section used for transverse collimation, at a location that has a high $D_x/\sqrt{\beta_x}$ value, where D_x and β_x are the longitudinal dispersion and betatron functions respectively. This location was chosen so that only particles with high energy deviation from the mean energy value will impact the primary collimator. Different locations for the secondary collimators were considered but although more than 80% of the input beam halo has been absorbed, in all cases there were losses that resulted in power deposition value significantly higher than the 1 W/m limit. It was found that the main reason these losses occur is the relatively short length of the secondary collimators, dictated by the space constraints of the arc. Further longitudinal collimation studies that include a change of the location of the primary and secondary collimators and the thickness of the primary collimator, are under investigation.

CONCLUSIONS AND FUTURE WORK

More than 96% of the inputed halo is absorbed by the collimators, however further improvements are necessary in order to be within the local beam loss limits. It was also shown that for different halo sizes the collimation-efficiency can change significantly.

It is essential that the collimation system will be further optimised in order to be within the radiation limits. Ongoing work that uses additional collimators showed promising results. Higher statistics should also be used as the number of particles has a direct effect on the accuracy of the efficiency. Additionally, the distribution used for the results presented in this paper is one of the worst-case scenarios since the particles occupy the largest possible horizontal and vertical phase-space; a different halo distribution will be generated that will represent a more realistic case. The longitudinal collimation studies will continue and finally, the impact of space-charge will be addressed in the immediate future.

ACKNOWLEDGMENT

The authors would like to thank J. Barranco and R. Bruce for the important input and valuable discussions.

REFERENCES

[1] Y. Papaphilippou et al., "Optics Design of the High-power Proton Synchrotron for LAGUNA-LBNO", IPAC'14, Dresden, Germany, June 2014, THPME068, These Proceedings.

[2] LAGUNA-LBNO Collaboration: Agarwalla, S. K. and others, "The mass-hierarchy and CP-violation discovery reach of the LBNO long-baseline neutrino experiment", arXiv:1312.6520 [hep-ph] (2013)

[3] J. B. Jeanneret, "Exact phase advances for optimum betatron collimation", LHC Project Note 116, November 1997

[4] SixTrack webpage: http://sixtrack.web.cern.ch

[5] "Tracking Code for Collimation Studies, extended version of SixTrack for collimation", http://lhc-collimation-project.web.cern.ch/lhc-collimation-project/code-tracking-2012.php

Content from this work may be used under the terms of the CC BY 3.0 licence (© 2014). Any distribution of this work must maintain attribution to the author(s), title of the work, publisher, and DOI.